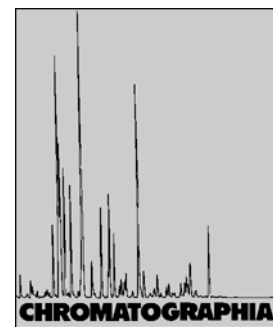


# Fabrication and Characterization of a Novel Biporous Spherical Adsorbent for Protein Chromatography



2003, 57, 29-35

Y. Shi / Y. Sun\*

Department of Biochemical Engineering, School of Chemical Engineering and Technology, Tianjin University, Tianjin 300072, P.R. China;  
E-Mail: ysun@tju.edu.cn

## Key Words

Column liquid chromatography  
Biporous matrix  
Radical suspension copolymerization  
Proteins

## Summary

A novel rigid spherical biporous poly(glycidyl methacrylate-triallyl isocyanurate-divinylbenzene) resin (denoted Resin B) has been fabricated by radical suspension copolymerization, with superfine granules of calcium carbonate, and toluene and *n*-heptane, as porogenic agents, as the basis of a novel porogenic mode, cooperation of solid granules and solvents. The pore structure, static adsorption behavior, and chromatographic properties of Resin B were characterized and compared with those of Resin A (with only solvents as porogens). The results indicated that the biporous resin is a promising chromatographic medium for high-speed protein separation with good mechanical performance and high dynamic adsorption capacity and column efficiency at high flow rates.

## Introduction

Liquid chromatography has proved a powerful technique for separation and purification of proteins, polypeptides, nucleic acids, polynucleotides, and other biomolecules [1]. A key aspect of liquid chromatography is choice of a suitable stationary phase. During the past decade continual efforts have been made to improve the separation of proteins by introducing new packing materials. Polymer-based porous resins are now preferred in downstream processing, because of their high mechanical strength, large binding capacity, and high chemical stability at high pH. For

conventional polymer-based porous media, however, slow mass transfer kinetics is the limiting factor that restricts the application of these supports to separations of biological macromolecules [2]. This undesired effect can be reduced by use of small non-porous particles. The very low loading capacity and low column permeability of non-porous particles has, however, made these columns less attractive for preparative-scale separations [3, 4].

Another solution is to increase bead permeability by use of wide pores connected to smaller diffusive pores. Examples include polystyrene materials such as POROS (PerSeptive Biosystems, USA)

with a bidisperse pore structure [5]. In contrast with conventional chromatographic packings, this so-called 'perfusible' polymeric biporous resin enables convective transport or less restricted diffusion of solutes in larger, interconnected pores and provides a substantial surface area as a result of the presence of smaller pores, and so resistance to stagnant mobile phase mass transfer is reduced significantly. The outstanding performance of this medium in the rapid separation of proteins has already been shown [6, 7]. New biporous matrices, prepared by in-situ copolymerization on the basis of the concept of a novel porogenic mode – the cooperation of solid granule and solvent – have recently been developed in our laboratory [8, 9]. The low mechanical stability of these irregularly-shaped media limits their use in high-speed protein chromatography, however.

Advances in suspension copolymerization technology have made it possible to prepare rigid polymeric resins with better mechanical and chemical stability, thus providing a new approach to the production of high-performance media for efficient chromatographic operations. In this paper we report the fabrication of a novel rigid biporous matrix (denoted Resin B), with granules of calcium carbonate, and toluene and *n*-heptane as porogenic agents, by radical suspension copolymerization. The pore structure, pore size distribution, specific surface area, water content, and static adsorption performance of Resin B have been determined and compared with those of Resin A, prepared with only solvents as porogens. The chro-

matographic properties were also investigated to find the differences between Resins A and B.

## Experimental

### Materials

Glycidyl methacrylate (GMA) (99%) was purchased from Suzhou Anli Chemical Company (Jiangsu, China) and used without further purification. Triallyl isocyanurate (TAIC) was purchased from Fluka (Buchs, Switzerland). Divinylbenzene (DVB; 45% divinyl monomer) from Shanghai Qunli Chemical Factory (Shanghai, China) was extracted with 10% aqueous sodium hydroxide and distilled water, dried over anhydrous magnesium sulfate, and distilled under vacuum. Toluene and *n*-heptane were both products of Tianjin Chemical Company (Tianjin, China). 2,2'-Azobis-(isobutyronitrile) (AIBN) was obtained from Tianjin Dagu Chemical Factory (Tianjin, China) and recrystallized from ethanol before use. Superfine calcium carbonate was purchased from Guangdong Enping Chemical Company (Guangping, China). All proteins used in this study were purchased from Sigma (St Louis, MO, USA), and dissolved in 0.01 M Tris-HCl buffer (pH 7.6). Other reagents were all of analytical grade and used as received.

### Synthesis of Polymer Matrices and Anion Exchangers

The poly(GMA-TAIC-DVB) beads were prepared by the radical suspension copolymerization method [10]. In general, the porogenic agents – solvents (toluene and *n*-heptane, 1.5:1 mol/mol) and/or granules of calcium carbonate – were added to a mixture of monomers (GMA, TAIC, and DVB, 1:0.17:0.17 mol/mol) in which the free radical initiator AIBN (2 mol% relative to the monomers) was dissolved. Compositions of the polymerization mixtures used to prepare Resins A and B were 100:67:0 and 100:67:40 (v/v; monomers-solvent-solid granule), respectively. After being degassed and well mixed in an ultrasonicator for 30 min the mixture was left for preliminary polymerization to increase the viscosity of the suspension. This reaction was performed at 40 °C in a shaking incubator (140 rpm) for 24 h. The mixture (20 mL) was then suspended in an

aqueous solution (100 mL) of 10 g L<sup>-1</sup> poly(vinyl alcohol) and 0.2 g L<sup>-1</sup> sodium lauryl sulfate, by agitation (500 rpm) under an atmosphere of nitrogen. The temperature used for suspension copolymerization was increased linearly from 45 to 65 °C within 1 h, then kept at 65 °C for 3 h, at 75 °C for 1 h, and finally at 85 °C for 2 h. The program of temperature changes was chosen to ensure that copolymerization did not occur too rapidly and to avoid the formation of bubbles in the beads. The resulting white beads were thoroughly washed with hot water. The solvent porogenic agents, toluene and *n*-heptane, were removed by extracting the beads with ethanol under reflux for at least 24 h, in a Soxhlet apparatus, whereas the solid porogenic agent, calcium carbonate, was removed by slow addition of 0.1 M hydrochloric acid solution to the solid suspension until no bubbles could be detected on addition of more hydrochloric acid. The beads were then washed thoroughly with distilled water and dried under vacuum (< 130 Pa) at room temperature.

For preparation of anion exchangers the beads were modified with diethylamine on the basis of a ring-opening reaction of the epoxide groups on the copolymer [10, 11]. Details for the procedure have been published elsewhere [9].

### Characterization of the Beads

Particle-size distributions of the resins were measured with a Mastersizer 2000 particle-size analyzer (Malvern Instruments, UK). Pore-size distribution analysis was performed with a Micromeritics Autopore II 9320 automated mercury porosimeter by mercury intrusion porosimetry. Scanning electron microscopy (SEM) was performed with an XL30 ESEM scanning microscope (Phillips, The Netherlands) to characterize the pore structures of the beads in the dry state. All samples were sputter-coated with gold before analysis. The specific surface area of the dry beads was determined by the three-point nitrogen adsorption (BET) method, with a BET ST-03 instrument. The water content of the resins was determined according to Wu and Brown [12]. The ion-exchange capacities of the resins were determined according to a method described elsewhere [10].

### Static Adsorption Isotherms

The standard batch adsorption system was used to determine the static adsorption isotherms of the anion exchangers, with bovine serum albumin (BSA) as model protein [13]. The initial BSA concentrations were from 0.2 to 2.0 mg mL<sup>-1</sup>. In a typical experiment, 0.05 g wet resin was mixed with 5.0 mL BSA solution of different concentrations for 24 h in a shaking incubator. At the end of adsorption the solid phase was centrifugally separated and the supernatant was analyzed at 280 nm for equilibrium liquid-phase protein concentration. The amount of protein adsorbed on the anion exchanger was calculated by mass balance.

### Chromatography

Beads of Resins A and B were packed into 30 or 100 mm × 4.6 mm i.d. stainless steel columns by means of an ethanol-slurry-packing technique. All packed-bed chromatography experiments were performed by use of an assembled Waters HPLC system consisting of a controller, a 600E pump, a manual injector with injector loops of 5 and 20 µL (Rheodyne 7725i, Australia), and a 2478 UV detector. Data acquisition and processing were performed with PC 800 software (Waters, Milford, MA, USA.).

The dynamic adsorption capacity was determined by frontal analysis. The column was equilibrated with approximately 10–15 column volumes (CV) of buffer A. After taking the column off-line the inlet capillary was purged with BSA solution (2 mg mL<sup>-1</sup>, 30 mL), and the detector was set to zero when the UV signal was stable. The column was then brought on-line and loaded with feed until the absorbance of the outlet stream had approached that of the inlet stream. The column was then eluted with NaCl (1 M, 30 CV) and re-equilibrated. On the basis of the UV signals obtained the level of breakthrough was determined by normalizing the protein concentration with the feed protein concentration. The dynamic capacity was calculated by use of Eq. (1):

$$q_{10} = [cF(t_{10} - t_0)]/V_B \quad (1)$$

where  $q_{10}$  is the dynamic capacity at 10% breakthrough,  $c$  is the concentration of BSA in the feed,  $t_{10}$  is the time of 10% breakthrough,  $t_0$  is the retention time under unretained conditions,  $F$  is volumetric flow rate, and  $V_B$  is the bed volume.

The column efficiency was expressed as the height equivalent to a theoretical plate ( $H$ ) [9]. Lysozyme was used as probe because it is positively charged in the buffer [14] and is, therefore, not adsorbed by the anion-exchange resin [8]. The experiments were conducted at flow velocities from 72 to 3240  $\text{cm h}^{-1}$ .

To compare the chromatographic separation performance of the bead-packed columns a protein mixture comprising BSA, hemoglobin, and lysozyme was used under identical chromatographic conditions. The ÄKTA FPLC system (Amersham Pharmacia Biotech, Uppsala, Sweden) was used for these experiments. Beads of resins A and B were packed into 50 mm  $\times$  5 mm i.d. Pharmacia HR5/5 glass columns with adjustable column tops; the columns were denoted HR Column-A and HR Column-B, respectively. Before sample injection, the columns were irrigated with buffer A for 15 CV. The injection volume was 25  $\mu\text{L}$ . After each run the column was eluted with NaCl (1.0 M, 10 CV). The column was then equilibrated with buffer A until a constant UV baseline was obtained.

## Results and Discussion

### Physical Properties of the Resins

The particle-size distributions of Resins A (prepared with solvents only as porogens) and B (prepared with solvents and calcium carbonate as porogens) are shown in Figure 1. For both resins the size distribution is narrow; the volume-weighted mean diameters of the resins are almost the same, 43.1  $\mu\text{m}$  for Resin A and 45.6  $\mu\text{m}$  for Resin B. Figure 2 shows SEM photographs of the resin beads. It can be seen that Resin A is strictly spherical and the surface of the beads is smooth and intact whereas Resin B contains regions of irregular macropores formed by the presence of the solid granules and numerous interconnected pores, typical of biporous polymer matrix.

Figure 3 depicts results from measurement of pore-size distribution. Here, the data are plotted as  $dV/d(\log D)$  (Figure 3a) and cumulative intrusion volume (Figure 3b) against pore diameter, where  $V$  is the volume of mercury that has penetrated and  $D$  is the pore diameter. Obviously, Resin A, prepared with the solvents as porogens, contains one family of pores in the range of approximately 10–

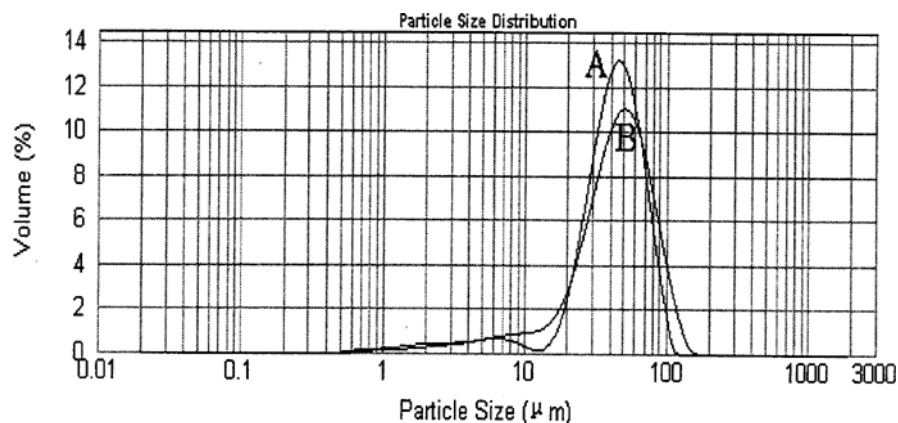
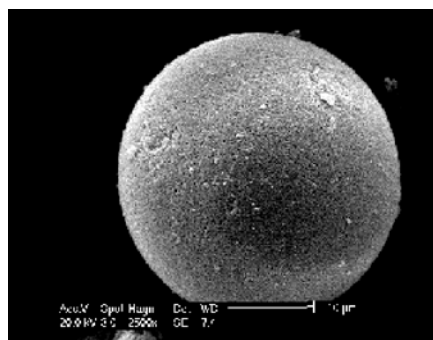
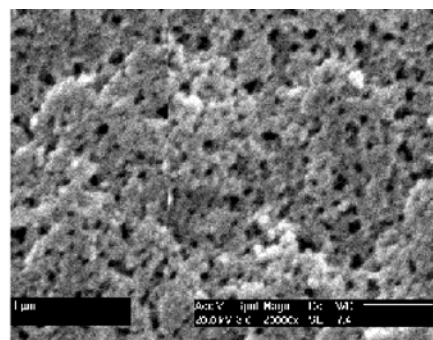


Figure 1. Particle-size distributions of the matrices.



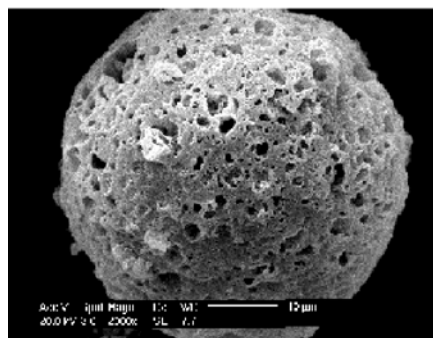
Resin A (2,500 X)

Acc V Spot Magn Det WD | -1 10  $\mu\text{m}$   
20.0 kV 3.0 2500x SE 74



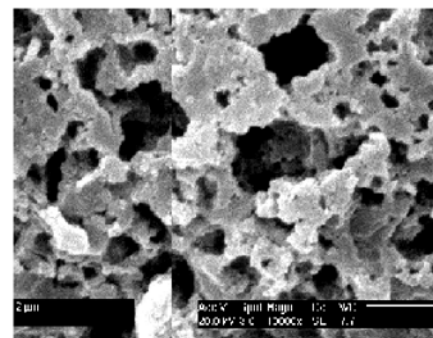
Resin A (20,000 X)

Acc V Spot Magn Det WD | -1 1  $\mu\text{m}$   
20.0 kV 3.0 20000x SE 74



Resin B (2,000 X)

Acc V Spot Magn Det WD | -1 10  $\mu\text{m}$   
20.0 kV 3.0 2000x SE 77



Resin B (10,000 X)

Acc V Spot Magn Det WD | -1 2  $\mu\text{m}$   
20.0 kV 3.0 10000x SE 77

Figure 2. Scanning electron micrographs of the matrices.

120 nm with a distinct maximum near 30 nm. In contrast, for Resin B, fabricated with both the solvents and solid granules as the porogens, a typical bimodal distribution is clearly apparent (Figure 3a). The large pores (300–4000 nm) might serve as intraparticle flow channels (as discussed below), and the population of small diffusive pores (approx. 10–150 nm) might contribute more significantly to the specific surface area. The pore-size

distribution of this resin can be explained in terms of the roles of the different porogenic agents. The liquid porogen is the main contributor to the regions of the micropores whereas the solid granules contribute to the macropore regions. Thus, the size of micropores and macropores in Resin B can be designed by adjusting the composition of the polymerization mixture [15] and the size of solid granules, respectively.

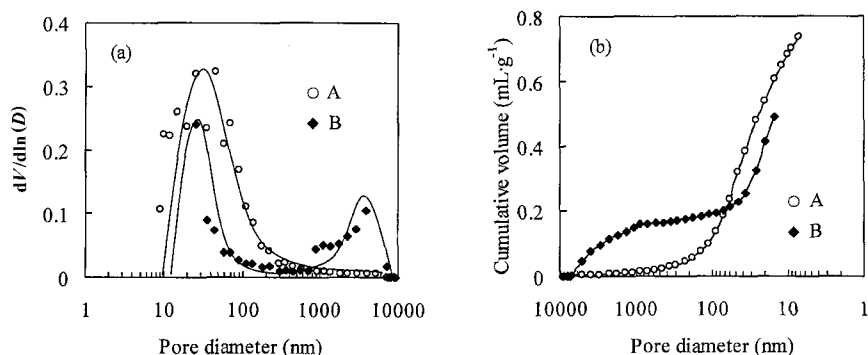


**Figure 3.** Pore-size distributions of the matrices for columns A and B: (a) incremental intrusion distribution; (b) cumulative intrusion distribution.

**Table I.** Physical properties of the resins.

Resin	$d_p$ ( $\mu\text{m}$ )	Specific surface area ( $\text{m}^2 \text{g}^{-1}$ )	Water content (% $w/w$ )	Hydrated density* ( $\text{g mL}^{-1}$ )	Ion-exchange capacity ( $\text{mmol g}^{-1}$ wet resin)
A	43.1	52.2	56.1	1.08	2.25
B	45.6	40.1	68.2	1.05	1.60

\* Measured with a 25-mL pycnometer.

In chromatography one demand on a stationary phase is high available particle surface area to enable a high binding capacity per unit volume of adsorbent bed, especially in preparative mode [16]. The specific surface areas of Resins A and B determined by BET were 52.2 and 40.1  $\text{m}^2 \text{g}^{-1}$ , respectively. In addition, the ion-exchange capacities of Resins A and B were estimated to be 2.25 and 1.60  $\text{mmol g}^{-1}$  wet resin, respectively. Compared with Resin A, the somewhat smaller specific surface and ion-exchange capacity of Resin B are because of the presence of macropores [16].

All the physical properties of the resins are summarized in Table I. It was found that the properties of resins prepared in different batches did not differ significantly.

## Protein Adsorption

### Static Adsorption Equilibrium

The static BSA adsorption isotherms of the anion-exchange resins are presented in Figure 4. The solid lines are calculated by use of the Langmuir equation:

$$q = q_m c / (K_d + c) \quad (2)$$

where  $q$  ( $\text{mg g}^{-1}$  wet resin) is the amount of BSA adsorbed by the adsorbent,  $q_m$  ( $\text{mg g}^{-1}$  wet resin) is the adsorption capacity,  $c$  ( $\text{mg mL}^{-1}$ ) is the equilibrium concentration of BSA in bulk solution, and

$K_d$  ( $\text{mg mL}^{-1}$ ) is the dissociation constant. The values of  $q_m$  and  $K_d$  were determined by fitting the equilibrium data to the Langmuir equation with the non-linear Simplex method. The static BSA capacities of Resins A and B were thus estimated to be 97.3 and 73.4  $\text{mg g}^{-1}$  wet resin, respectively. Using the data for the hydrated density of Resin B (Table I) and assuming a packed-bed voidage of 0.40 [17], it was estimated that the capacity of Resin B is 47.1  $\text{mg mL}^{-1}$  bed column. This capacity value compares favorably with those of commercially available biporous anion-exchangers for the same model protein [18].

### Dynamic Binding Capacity

Breakthrough curves provide information about the dynamic binding capacity of a separation medium, which is extremely important for large-scale separations. The discrepancy between the static and dynamic binding capacities of an adsorbent is a sensitive measure of mass-transfer limitations [19, 20]. Figure 5 illustrates BSA breakthrough curves at 180  $\text{cm h}^{-1}$  for Columns A and B. The 10% breakthrough adsorption capacity of Column A is only 4.6  $\text{mg mL}^{-1}$  column bed (or 7.1  $\text{mg g}^{-1}$  wet resin) whereas for Column B a capacity of 34.6  $\text{mg mL}^{-1}$  column bed (or 54.9  $\text{mg g}^{-1}$  wet resin = 57.7  $\text{mg mL}^{-1}$ ) is obtained. The dynamic capacity of Column A was substantially lower than the static capacity determined by batch

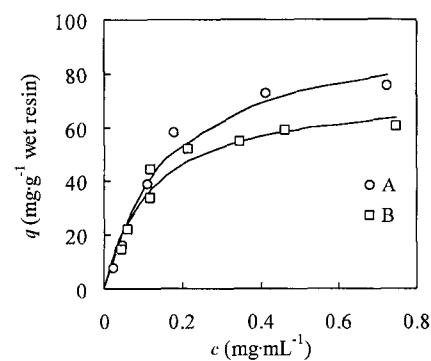


**Figure 4.** Static adsorption isotherms for adsorption of BSA by the anion-exchange resins in columns A and B.

experiments, which enabled saturation of the binding sites. This is because of the intrinsically low intraparticle diffusive mass transfer of the macromolecules in Resin A. The dynamic capacity of Resin B, on the other hand, was approximately 75% of its static capacity, which proves that BSA molecules permeate the particles of Resin B, by a combination of convective and diffusive mass transport, because of the presence of the flow-through macropores, and thus the rate of mass transfer is accelerated.

To confirm further the conclusion that intraparticle mass transfer in Resin B is greatly enhanced by convection, the dynamic adsorption capacities of Resins A and B were measured at elevated flow rates. The effect of flow rate on the 10% breakthrough capacities for adsorption of BSA on Resins A and B is shown in Figure 6. It is clearly apparent that for Column B convective intraparticle mass transfer dominated [21] and the dynamic capacity decreased by only approximately 17% when the flow rate was increased from 180 to 1800  $\text{cm h}^{-1}$ . At a superficial velocity of 1800  $\text{cm h}^{-1}$  the dynamic capacity of Resin B remained at 64% of its saturation capacity.

It has been reported that the dynamic capacity (at 10% breakthrough) of the commercially available biporous polymer-based anion-exchange resin POROS QE/M for BSA was 38  $\text{mg mL}^{-1}$  at a flow rate of 720  $\text{cm h}^{-1}$ ; this is lower than those of TSK-Gel-Q-5PW-HR, Express-Ion Q,

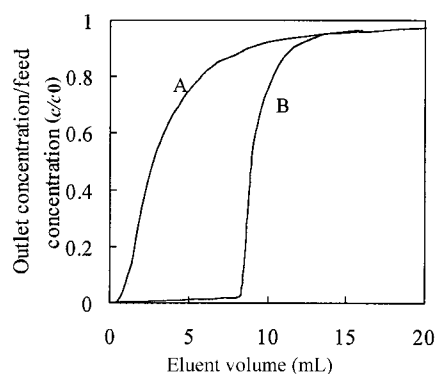


**Figure 5.** Breakthrough curves for BSA on columns A and B at  $180 \text{ cm h}^{-1}$ . Conditions:  $30 \text{ mm} \times 4.6 \text{ mm}$  i.d. column; mobile phase  $0.01 \text{ M}$  Tris-HCl buffer, pH 7.6; feed BSA concentration  $2 \text{ mg mL}^{-1}$ ; UV detection at  $280 \text{ nm}$ .

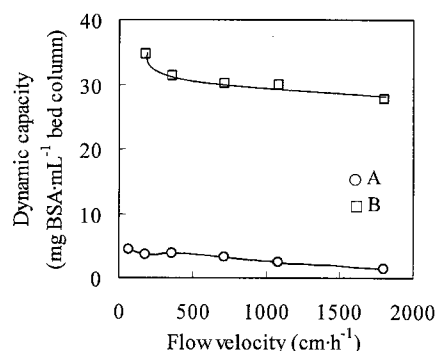


**Figure 6.** Dynamic capacity of BSA on columns A and B at 10% breakthrough as a function of flow velocity.

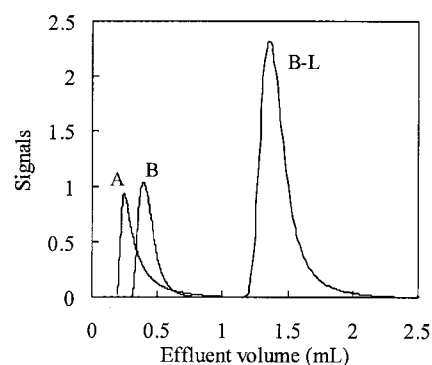


**Figure 7.** Chromatograms of lysozyme obtained from columns A and B. Experiments were performed at  $1800 \text{ cm h}^{-1}$ . Conditions: UV detection at  $280 \text{ nm}$ ; mobile phase  $0.01 \text{ M}$  Tris-HCl buffer, pH 7.6; feed lysozyme concentration  $5 \text{ mg mL}^{-1}$ ; columns A and B  $30 \text{ mm} \times 4.6 \text{ mm}$  i.d.; injection volume  $5 \mu\text{L}$ ; column B-L  $100 \text{ mm} \times 4.6 \text{ mm}$  i.d.; injection volume  $20 \mu\text{L}$ .

and Q Sepharose FF (42, 50, and  $54 \text{ mg mL}^{-1}$ , respectively) [22]. Obviously, Resin B has a dynamic binding capacity higher than that of this biporous resin and TSK-Gel-Q-5PW-HR, and comparable with those of Express-Ion Q and Q Sepharose FF.

## Elution Chromatography of Lysozyme

### Elution Peaks

To investigate the effect of column length on the efficiency of columns packed with Resin B the resin was also packed into a longer column ( $100 \text{ mm} \times 4.6 \text{ mm}$  i.d., denoted Column B-L). For this column the injection volume was  $20 \mu\text{L}$ , instead of the typical  $5 \mu\text{L}$  injection size for the other columns. Figure 7 shows the chromatographic peaks obtained for elution of lysozyme from Columns A, B, and B-L at a mobile phase flow rate of  $1800 \text{ cm h}^{-1}$ .

The extra-column contribution to band broadening is negligible, because the volumes of the extra-column tubing and fittings are much smaller than the widths of the observed peaks [23]. It has also been well documented that the rate of mass transport of proteins to interior binding sites is typically the dominant contribution to band broadening [19]. Obviously, the tailing peak for Column A can be attributed to the high intraparticle mass-transfer resistance. In contrast, band broadening was not so significant for elution from Columns B and B-L as for elution from Column A. This is largely be-

cause of the enhanced intraparticle mass transport of protein molecules, because of the presence of flow-through macropores in Resin B.

### Column Efficiency

Column efficiency is an important criterion for evaluating the performance of chromatographic columns, particularly for columns packed with polymer-based packing materials, because it is well understood that polymer-based HPLC packing materials have inherently lower column efficiency [24]. The column efficiency of the resins as a function of flow rate are depicted in Figure 8. It is apparent that Columns B and B-L were much more efficient than Column A. The  $H$  values of Columns B and B-L were, moreover, almost unchanged in the range of mobile phase velocities below  $1800 \text{ cm h}^{-1}$  whereas a linear increase of plate height with flow rate was observed for Column A. This behavior is ascribed to the different mass-transfer mechanisms. Mass transfer in Resin A is diffusion-limited, so there is more diffusive resistance in Resin A and column efficiency decreases with increasing the mobile phase flow rate [25]. On the other hand, accelerated mass transfer resulting from the presence of the flow-through pores in Resin B (diffusion-convection) substantially reduces the negative effect of micropore diffusion on plate height, enabling transport of molecules into the interior of the particle by convective flow. Improved column performance is therefore obtained from Resin B because the  $H$  value is less than that

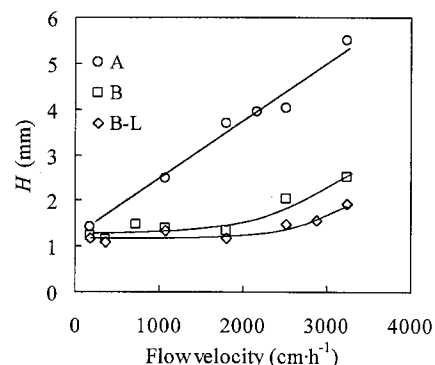


**Figure 8.** Column efficiency for lysozyme as a function of mobile phase flow rate for columns A, B, and B-L. Conditions as for Figure 7.

for Resin A. The speed of separation can, moreover, be increased without loss of column efficiency [26–28].

It is also apparent from Figure 8 that the efficiency of Column B-L was higher than that of Column B over the entire flow rate range tested. It is likely that the lower efficiency of Column B is because of the larger contribution of the end effect in the short column [29].

It has been reported that plate heights for lysozyme of columns packed with  $21.8 \mu\text{m}$  POROS 20SP and  $26.6 \mu\text{m}$  SP POROS 20 OH beads under unretained conditions were  $0.87$  and  $1.20 \text{ mm}$ , respectively, at  $1222 \text{ cm h}^{-1}$  [16], and that the value for myoglobin of the column packed with  $20 \mu\text{m}$  POROS QE/M beads was approximately  $2 \text{ mm}$  at  $720 \text{ cm h}^{-1}$  [22]. The results presented here all indicate that column efficiency for Resin B was comparable with those of the commercially available biporous polymeric media of smaller particle size.

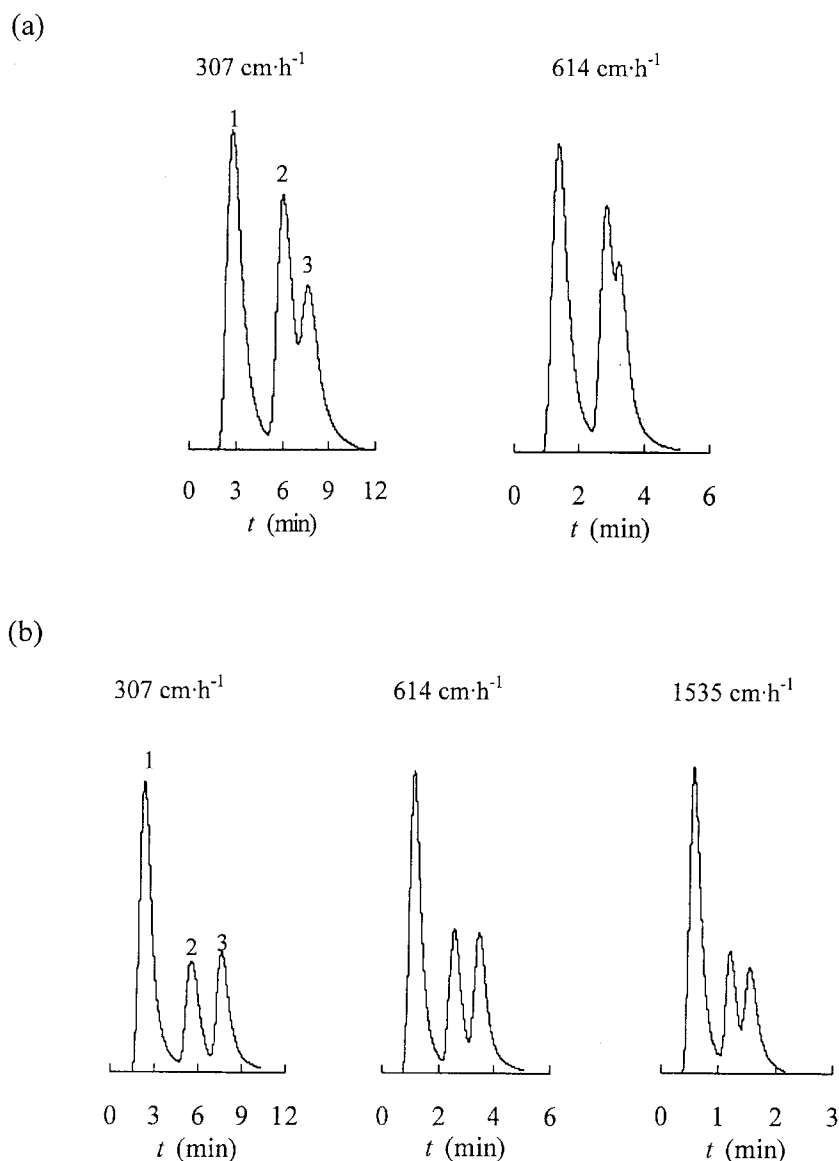


**Figure 9.** Separation of (1) lysozyme, (2) hemoglobin, and (3) BSA on (a) HR Column-A and (b) HR Column-B. Experimental conditions: buffer A, 0.01 M Tris-HCl buffer (pH 7.6); buffer B, 0.3 M NaCl in buffer A (pH 7.6); injection size, 25  $\mu$ L; gradient 100% buffer A in 2 mL, 0–100% buffer B in 10 mL; protein concentrations: lysozyme 5 mg mL<sup>-1</sup>, hemoglobin 5 mg mL<sup>-1</sup>, BSA 10 mg mL<sup>-1</sup>; UV detection at 280 nm.

### Separation of Protein Mixtures

Gradient elution chromatography was performed to assess the suitability of the resins for protein separation. The gradient was run from 0 to 0.3 M NaCl; the chromatographic separations obtained are shown in Figure 9. These results indicate that, because of the presence of the flow-through pores, HR Column-B enabled complete separation of the three components of the mixture, and that increasing the flow rate to 1535 cm h<sup>-1</sup> barely reduced the resolution. For HR Column-A, however, the resolution decreased significantly when the flow rate was increased to 614 cm h<sup>-1</sup>. Combined

with the results from determination of column efficiency (Figure 8), it can be concluded that the mass transfer limitation of the porous resins has been minimized by introducing flow-through pores.

### Conclusions

In previous work we developed a novel porogenic mode – cooperation of solid granules and solvents – which simplifies the preparation of biporous media by simple in-situ copolymerization. In the work discussed in this paper a biporous copolymer of GMA, DVB, and TAIC was produced by suspension copolymerization

using granules of calcium carbonate, and toluene and *n*-heptane, as porogenic agents. The solid phase was used as an anion exchanger after functionalization with diethylamine. Results from SEM and mercury intrusion porosimetry revealed that the matrix contains regions of micropores (approx. 10–150 nm) and regions of macropores (approx. 300–4000 nm). Result from BET experiments show that the biporous medium had a high specific surface area – 40.1 m<sup>2</sup> g<sup>-1</sup>. Experiments revealed that columns packed with this biporous medium can be operated at mobile flow rates as high as 3241 cm h<sup>-1</sup>, indicating good mechanical performance. Because of the presence of flow-through pores, the dynamic adsorption capacity was as high as 53.9 mg g<sup>-1</sup> wet resin, approximately 75% of its static capacity. In addition, columns packed with this material were highly efficient, as determined with lysozyme as model protein. Separations of proteins on this column revealed that resolution did not decrease at linear flow rates up to 1535 cm h<sup>-1</sup> – the results showed that the flow-through pores in the biporous resin substantially increase the rate of mass transfer of the large molecules and minimize the negative effects of diffusion. These characteristics make this biporous matrix useful for high-speed chromatographic purification of proteins.

### Acknowledgment

This research was supported by the National Natural Science Foundation of the P.R. China.

### References

- [1] Zeng, X.; Ruckenstein, E. *J. Membrane Sci.* **1998**, *148*, 195–205.
- [2] Garcia, M.C.; Marina, M.L.; Torre, M. *J. Chromatogr. A* **2000**, *880*, 169–187.
- [3] Horváth, J.; Boschetti, E.; Guerrier, L.; Cooke, N. *J. Chromatogr. A* **1994**, *679*, 11–22.
- [4] Tennikov, M.B.; Gazdina, N.V.; Tennikova, T.B.; Svec, F. *J. Chromatogr. A* **1998**, *798*, 55–64.
- [5] Afeyan, N.B.; Gordon, N.F.; Mazasaroff, I.; Varady, L.; Fulton, S.P.; Yang, Y.B.; Regnier, F.E. *J. Chromatogr.* **1990**, *519*, 1–29.
- [6] Carta, G.; Rodrigues, A.E. *Chem. Eng. Sci.* **1993**, *48*, 3927–3935.
- [7] Frey, D.; Schwesheim, E.; Horváth, Cs. *Biotechnol. Prog.* **1993**, *9*, 93–100.
- [8] Zhang, M.L.; Sun, Y. *J. Chromatogr. A* **2001**, *922*, 77–86.

- [9] Shi, Y.; Dong, X.-Y.; Sun, Y. *Chromatographia* **2002**, *55*(7/8), 405–410.
- [10] Yu, Y.H.; Sun, Y. *J. Chromatogr. A* **1999**, *855*, 129–136.
- [11] Zhou, X.; Xue, B.; Sun, Y. *Biotechnol. Prog.* **2001**, *17*, 1093–1098.
- [12] Wu, G.; Brown, G.R. *React. Polym.* **1991**, *14*, 49–61.
- [13] He, L.Z.; Gan, Y.R.; Sun, Y. *Bioprocess Eng.* **1997**, *17*(5), 301–305.
- [14] Keggubgerm, A.L. *Principles of Biochemistry*, Worth, New York, **1982**.
- [15] Guyot, A.; Bartholin, M. *Prog. Polym. Sci.* **1982**, *8*, 277–331.
- [16] Nash, D.C.; Chase, H.A. *J. Chromatogr. A* **1998**, *807*, 185–207.
- [17] Boyer, P.M.; Hsu, J.T. *AIChE J.* **1992**, *38*, 259–272.
- [18] Levison, P.R.; Mumford, C.; Streater, M.; Brandt-Nielsen, A.; Pathirana, N.D.; Badger, S.E. *J. Chromatogr. A* **1997**, *760*, 151–158.
- [19] Van Deemter, J.J.; Zuiderweg, F.J.; Klinkenberg, A. *Chem. Eng. Sci.* **1956**, *5*, 271–289.
- [20] Deen, W.M. *AIChE J.* **1987**, *33*, 1409–1425.
- [21] Nash, D.C.; Chase, H.A. *J. Chromatogr. A* **1997**, *776*, 65–73.
- [22] Staby, A.; Jensen, I.H.; Mollerup, I. *J. Chromatogr. A* **2000**, *897*, 99–111.
- [23] Gowanlock, D.; Bailey, R.; Cantwell, F.F. *J. Chromatogr. A* **1996**, *726*, 1–23.
- [24] Yang, Y.B.; Harrison, K.; Kindsvater, J. *J. Chromatogr. A* **1996**, *723*, 1–10.
- [25] Rendueles de la Vega, M.; Chenou, C.; Loureiro, J.M.; Rodrigues, A.E. *Biochem. Eng. J.* **1998**, *1*, 11–23.
- [26] Afeyan, N.B.; Fulton, S.P.; Regnier, F.E. *J. Chromatogr.* **1991**, *544*, 267–279.
- [27] Liapis, I.; McCoy, M.A. *J. Chromatogr.* **1992**, *599*, 87–104.
- [28] Rodrigues, A.E. *J. Chromatogr. B* **1997**, *699*, 47–61.
- [29] Koh, J.-H.; Guiochon, G. *J. Chromatogr. A* **1998**, *796*, 41–57.

Received: Jul 19, 2002

Revised manuscript

received: Sep 4, 2002

Accepted: Sep 13, 2002